

Structural analysis of kasugamycin inhibition of translation

Barbara S Schuwirth^{1,5}, J Michael Day^{2,5}, Cathy W Hau^{1,5}, Gary R Janssen², Albert E Dahlberg³, Jamie H Doudna Cate^{1,4} & Antón Vila-Sanjurjo^{1,4,5}

The prokaryotic ribosome is an important target of antibiotic action. We determined the X-ray structure of the aminoglycoside kasugamycin (Ksg) in complex with the *Escherichia coli* 70S ribosome at 3.5-Å resolution. The structure reveals that the drug binds within the messenger RNA channel of the 30S subunit between the universally conserved G926 and A794 nucleotides in 16S ribosomal RNA, which are sites of Ksg resistance. To our surprise, Ksg resistance mutations do not inhibit binding of the drug to the ribosome. The present structural and biochemical results indicate that inhibition by Ksg and Ksg resistance are closely linked to the structure of the mRNA at the junction of the peptidyl-tRNA and exit-tRNA sites (P and E sites).

Translation initiation is the rate-limiting step of protein synthesis and is a central target for the global regulation of gene expression¹. In bacteria, modulation of translation initiation has been attributed to sequences and secondary structures within mRNAs. These include the strength of the Shine-Dalgarno (SD) sequence, the identity of the initiation codon, the presence or absence of secondary structures in the 5' leader sequence and the presence of A/U-rich sequences recognized by ribosomal protein S1 (refs. 2,3). However, the role of the sequence between the SD and the initiation codon remains unclear, despite reports showing large effects of this region on gene expression^{2,4,5}. This stretch of mRNA traverses the universally conserved ribosomal E site within the 30S subunit during initiation^{6,7}.

The aminoglycoside Ksg has been reported to inhibit initiation of translation by blocking initiator transfer RNA binding to the 30S subunit^{8–12}. Ksg is produced by the bacterium *Streptomyces kasugaensis*¹³ and has been used clinically in the treatment of *Pseudomonas aeruginosa* infections¹⁴. The antibiotic is currently used in the treatment of the fungus *Pyricularia oryzae* in rice fields¹³.

As with nearly all classes of antibiotic, resistance mutations have been found for Ksg. Resistance to Ksg was first mapped to the *ksgA* gene¹⁵. *ksgA* encodes a methyltransferase that catalyzes the post-transcriptional dimethylation of N6 of A1518 and A1519 in the loop that closes helix 45 near the 3' end of 16S rRNA (dimethyl-A stem-loop or DASL; Fig. 1a)^{16,17}. Lack of modification in this stem-loop leads to Ksg resistance¹⁶. Although the role of this modification is unknown, both the KsgA methyltransferase and its target seem to be

conserved throughout evolution¹⁸. More recently, Ksg resistance mutations have been isolated in 16S rRNA at position A1519 and at the universally conserved residues A794 and G926 (Fig. 1a)¹⁹. Chemical probing of wild-type ribosomes with Ksg changes the reactivity of A794, C795 and G926, suggesting that these residues are involved in binding the drug²⁰. These residues map to the cleft between the head and the platform of the 30S subunit, near the pathway of mRNA in the ribosomal E site (Fig. 1b)^{6,7}.

We decided to investigate the Ksg binding site on the ribosome by means of X-ray crystallography. The 3.5-Å structure of the *E. coli* 70S ribosome in complex with Ksg described here reveals that the drug occupies the mRNA channel between the ribosomal P and E sites. In addition, biochemical experiments show that the identities of the mRNA residues located between –2 and +1 (where –1 is the last position of the E-site codon and +1 is the first position of the P-site codon) have a large effect on the extent of inhibition by Ksg. Ksg therefore acts as a selective inhibitor of a subset of mRNAs by interfering with the path of mRNA immediately upstream of the start codon. These results offer, for the first time, an explanation for both the mode of action of Ksg and the important role of the E site in gene expression.

RESULTS

Ksg binds the 30S subunit

The structure of Ksg bound to the *E. coli* 70S ribosome was determined by X-ray crystallography (Fig. 1). Ksg was soaked into

¹Departments of Molecular and Cell Biology and Chemistry, University of California, Berkeley, California 94720, USA. ²Department of Microbiology, Miami University, Oxford, Ohio 45056, USA. ³Department of Molecular Biology, Cell Biology and Biochemistry, Brown University, Providence, Rhode Island 02912, USA. ⁴Physical Biosciences Division, Lawrence Berkeley National Laboratory, Berkeley, California 94720, USA. ⁵Present addresses: Cancer research UK London Research Institute, Clare Hall Laboratories, South Mimms, Hertfordshire EN6 3LD, UK (B.S.S.), US Department of Agriculture, Agricultural Research Service, SEPRL 934 College Station Road, Athens, Georgia 30605, USA (J.M.D.), Department of Anesthesia, University of California, San Francisco, California 94143, USA (C.W.H.) and Berkeley Center for Synthetic Biology, University of California, 717 Potter St., Berkeley, California 94720-3224, USA (A.V.S.). Correspondence should be addressed to J.H.D.C. (jcate@lbl.gov) and A.V.S. (avila@lbl.gov).

Received 6 June; accepted 31 August; published online 24 September 2006; doi:10.1038/nsmb1150

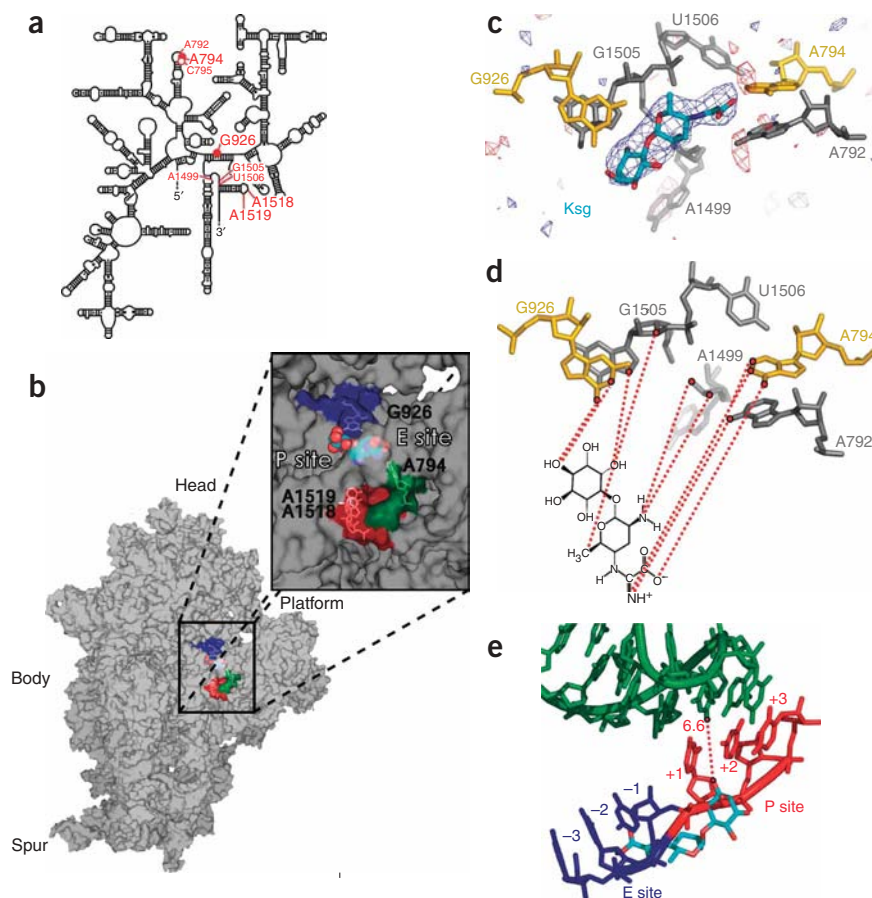


Figure 1 Location of the Ksg-binding pocket in the ribosome. (a) Secondary structure of 16S rRNA, showing the resistance sites (large characters) and residues in contact with Ksg (small characters). Sites of altered reactivity toward chemical probes in the presence of Ksg are shown as filled circles (protections) or empty circles (enhancements). (b) The Ksg-binding pocket in the context of the 30S subunit, highlighting Ksg (cyan), the 790 loop (green), the 926 region (blue) and the DASL (red). Residues A794, G926, A1518 and A1519 are shown as sticks. (c) Close-up view of the Ksg-binding pocket of 30S-1 showing Ksg (cyan) docked into the positive electronic density (blue mesh). Also shown: negative electronic density (red), resistance sites (gold) and contact sites (gray). (d) Contact sites, color-coded as in c. (e) Location of Ksg relative to P-site tRNA and mRNA. Shown are Ksg (cyan), P-site mRNA (red), E-site mRNA (blue), anticodon stem-loop (green). mRNA residues are labeled with position relative to first base of P-site codon (+1). ASL and mRNA coordinates were extracted from the structure of the *T. thermophilus* 30S subunit (PDB entry 1FJG)⁶.

near the Ksg electron density are A792, A1499, G1505 and U1506 (Fig. 1c,d and Supplementary Fig. 1).

Ksg consists of an acetamidinium-carboxylate group attached to a hexopyranosyl ring and an inositol ring (Fig. 1d). In the refined structure, the inositol ring packs against the bases of G926 and G1505, which are stacked. The O4- and O2-hydroxyls on the inositol ring are within hydrogen-bonding distance of the N1 of G926 and N7 of G1505, respectively (Fig. 1d). The hexopyranosyl ring of Ksg bridges the backbones of 16S rRNA nucleotides in the loop closed by bases A1499 and U1506. The hexopyranosyl methyl group may pack against the ribose C3' atom of G1505, whereas the amine makes direct contacts with the phosphate of A1499 (Fig. 1d). The acetamidinium-carboxylate functional group of Ksg makes a number of contacts that are probably part of a water-mediated hydrogen bond network. In both ribosomes, the carboxy-imino N3 of Ksg is within hydrogen-bonding distance of the N1 of A794 and within van der Waals distance of the C2 of A794 (Fig. 1d). The same atom of Ksg is also within van der Waals distance of the N6 of A792 in 30S-1 and possibly in 30S-2. An additional hydrogen bond may exist between the carboxyl group of Ksg and the N6 of A794 (Fig. 1d).

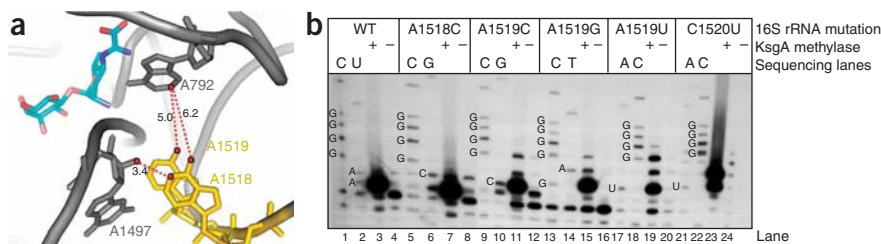
Ksg protects nucleotides A794 and G926 from modification by chemical probes²⁰. These residues are also protected by binding of P-site tRNA to the ribosome²². However, docking of P-site tRNA or its analog from structures of the 30S subunit and 70S ribosome^{6,23} into our structure reveals that the P-site tRNA and Ksg are separated by more than 6 Å (Fig. 1e). A direct contact between Ksg and P-site tRNA therefore seems unlikely to contribute to inhibition of initiation. The position of Ksg within the mRNA channel suggests that the drug may actually interfere with mRNA binding to the ribosome (Fig. 1b)^{6,7}. Indeed, docking of an mRNA analog in the 30S subunit⁶ or mRNAs from 70S ribosome structure^{7,23} into the 70S ribosome–Ksg structure suggests that a steric clash would exist between Ksg and the mRNA backbone between positions –2 and +1 (Fig. 1e).

ribosome crystals grown under conditions recently reported²¹. We measured diffraction data from crystals of the ribosome–Ksg complex to 3.5 Å and created an ($F_o - F_c$) difference electron density map, obtaining control structure factors from the apo-70S ribosome structure (Supplementary Table 1 online)²¹. The difference map revealed positive difference density, easily attributable to Ksg, in the two small subunits contained in the asymmetric unit of the crystals (herein named 30S-1 and 30S-2). The density was located in the mRNA channel between the head and the platform of the subunit (Fig. 1b). Manual docking of the Ksg molecule into the difference electron density relied on unique features of the electron density. For example, the shape of the electron density positions the acetamidinium-carboxylate group uniquely near A794, given the size of the density surrounding the inositol ring (Fig. 1d). Moreover, the asymmetric linkage between the acetamidinium-carboxylate group and the hexopyranose ring, relative to the methyl and amino groups, could be discerned clearly as a 'bump' in the electron density (Fig. 1c). Crystallographic refinement of Ksg bound to the two 70S ribosomes was performed as described in Methods.

Ksg binds within the mRNA channel

The Ksg-binding pocket is composed entirely of 16S rRNA residues that line the mRNA channel of the small subunit, located between the universally conserved A794 and G926 (Fig. 1b–d and Supplementary Fig. 1 online)^{6,7}. This agrees perfectly with Ksg protection of these two residues from chemical probes²⁰ and with high levels of Ksg resistance conferred by base changes at these positions¹⁹. Additional nucleotides

Figure 2 Determinants of resistance to Ksg in the DASL. (a) Location of the DASL relative to Ksg. DASL residues A1518 and A1519 are shown (gold). Also shown are A792 and G1497 (gray), Ksg (cyan) and distances from the DASL to these residues (in Angstroms). (b) Post-transcriptional modification of the DASL. Plasmid-encoded 16S rRNAs carrying mutations in the DASL (or wild-type (WT) rRNAs) were isolated from *ksgA*⁺ (lanes 3, 7, 11, 15, 19 and 23) or *ksgA*⁻ strains (lanes 4, 8, 12, 16, 20 and 24). The presence of the methyl groups at A1518 and/or A1519 in 16S rRNA is detected as a strong reverse-transcriptase stop in primer extension¹⁹. Sequencing lanes, containing rRNA isolated from the *ksgA*⁻ strain, are included for every mutant.



Location of Ksg relative to the DASL

Despite the fact that lack of methylation of 1518 and 1519 in the DASL leads to Ksg resistance^{16,19}, this stem-loop does not contact Ksg directly (Fig. 2a). This may explain why lack of methylation or mutations in this loop confer only a low level of resistance¹⁹. Nucleotides m²A1518 and m²A1519 are buried in a pocket between the 790 loop and the 1500 region of helix 44 (Fig. 2a). Notably, the N6 group of m²A1519 is much closer to A792 than that of m²A1518 (5 Å versus ~6.2 Å for m²A1519 and m²A1518, respectively) and could place one of the methyl groups close enough for van der Waals contact with C2 of A792 (Fig. 2a and Supplementary Fig. 1). Mutation of m²A1519 by itself confers as much resistance to Ksg as do *ksgA* mutations, whereas mutation of m²A1518 confers no resistance¹⁹. These results indicate that the identity of position 1518 and its methylation status are not determinants of resistance to Ksg.

On the basis of the above structural and genetic results, we reasoned that disruption of the packing of A792 with m²A1519—that is, the absence of A1519 methylation—should be sufficient to confer weak resistance. In other words, Ksg-sensitive ribosomes carrying a mutation at position 1518 would still be methylated at the adjacent A1519, and resistance mutations at position 1519 would not necessarily interfere with methylation at A1518. Accordingly, primer-extension analysis of 16S rRNA revealed that mutation of either adenosine did not affect the methylation of the adjacent nucleotide by KsgA (Fig. 2b)^{19,24}. Even mutation of the neighboring C1520 to U²⁵ did not prevent the methylation of A1518 and A1519 (Fig. 2b). Together, these data indicate that the only change in the DASL required for resistance to Ksg is demethylation of the N6 group of m²A1519.

Kasugamycin binds mutant ribosomes *in vitro*

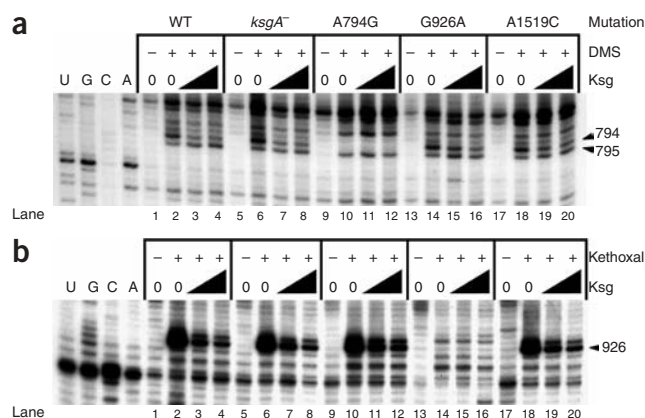
Ksg resistance could be explained by a loss of affinity of 30S subunits for the drug. Binding of Ksg to wild-type 30S subunits protects residue A794 from modification by dimethyl sulfate (DMS) and G926 from modification by kethoxal, and enhances the DMS reactivity of C795 (ref. 20). Notably, ribosomes from wild-type and *ksgA*⁻ cells have very similar protection patterns at A794, C795 and G926 induced by Ksg (Fig. 3a,b and Supplementary Table 2 online), suggesting that Ksg

binding to these 30S subunits is not substantially impaired within the concentration range tested. The footprint at G926 was consistently more intense than that at A794, perhaps reflecting a tighter contact of the drug with the former residue. The results obtained with the A1519C mutation deserve particular attention. Although decreased protection by Ksg at A794 was consistently observed for this mutant, the strength of protection of G926 was similar to that obtained with wild-type ribosomes, indicating that the A1519C resistance mutation does not considerably impair Ksg binding (Fig. 3b and Supplementary Table 2). The reduced Ksg footprint in the 794 region for this mutant is consistent with a structural change in this region in response to the A1519C mutation (Fig. 3a and Supplementary Table 2). It is noteworthy that the extent of protection in the highly resistant mutants (A794G and G926A; Fig. 3a,b and Supplementary Table 2), for which only one footprint site is available for analysis, seems to be slightly decreased. This finding suggests that these two mutations result in a slightly lower affinity of the ribosomes for the drug.

Ksg can inhibit all mutant ribosomes

To determine more precisely which step of initiation Ksg inhibits, toeprinting experiments were carried out to detect the extent of tRNA^{fMet} binding to wild-type and mutant ribosomes. Ksg has been shown to bind 30S subunits from *ksgA* mutants and inhibit the binding of fMet-tRNA^{fMet} in the presence of initiation factors (IFs)¹⁰. In toeprint experiments with 30S subunits in the presence of a T7-transcribed leaderless mRNA and IF2-GTP-fMet-tRNA^{fMet}, Ksg blocked the mRNA-tRNA^{fMet} interaction in all the Ksg-resistant 30S subunits (Fig. 4a and Supplementary Table 3 online). Notably, ribosomes from *ksgA* mutants seem to be much more resistant to the drug than the other mutants in this assay, consistent with the distance of the dimethyl-A (m²A) stem-loop from the antibiotic-binding site. This experiment confirmed that Ksg binds all the Ksg-resistant 30S

Figure 3 Chemical modification of mutant and wild-type 30S subunits in the presence of Ksg. Sequencing lanes are labeled U, G, C and A. (a) Ksg footprint in the 794 region of the 16S rRNA upon chemical modification with DMS. (b) Ksg footprint in the 926 region of the 16S rRNA upon chemical modification with kethoxal. The A794G mutation renders the DMS reactivity of this base undetectable, and the G926A mutation makes this residue unreactive to chemical attack by kethoxal; thus, Ksg binding to ribosomes carrying a mutation at one residue was detected as protection of the other residue. Ksg was used at 0, 64 and 320 μg ml⁻¹ (triangles denote increasing concentration). WT, wild-type rRNA.



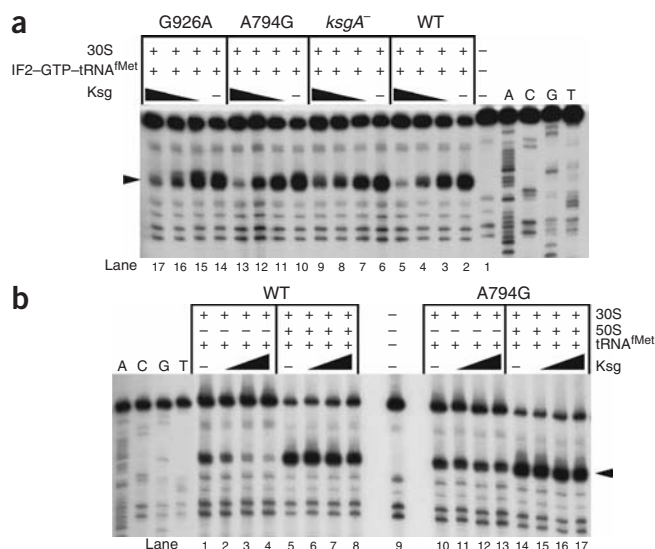


Figure 4 Toeprint experiments with leaderless mRNA. **(a)** Effect of Ksg on the IF2-mediated binding of fMet-tRNA^{fMet} to 30S subunits in the presence of LL mRNA. Reaction components are indicated above lanes; Ksg was preincubated with ribosomes at 100, 500 and 1,000 $\mu\text{g ml}^{-1}$ (triangles denote increase). **(b)** Effect of Ksg on initiation-complex formation on LL mRNA in the presence of deacylated tRNA^{fMet}. Reaction components are indicated above lanes, with Ksg preincubated as in **a**. Arrowheads indicate position of toeprint. Sequencing lanes are labeled A, C, G and U.

subunits, thus extending previously published results¹⁰. However, a different picture was obtained in toeprint experiments without IFs and in the presence of deacylated initiator tRNA^{fMet}. Contrary to the situation when IFs are present, initiator tRNA binds directly at the classical P site in their absence²². Although the wild-type 30S subunits retained their sensitivity to Ksg, all the mutant 30S subunits were considerably more resistant to the drug than in the presence of IFs (Fig. 4b, Supplementary Table 3 and data not shown). The sensitivity of the wild-type subunits disappeared when 50S subunits were added to the reaction (Fig. 4b and Supplementary Table 3), consistent with previous reports describing the Ksg resistance of 70S ribosomes programmed with leaderless mRNAs²⁶. Moreover, addition of 50S subunits further increased the resistance of the A794G ribosomes (Fig. 4b and Supplementary Table 3). Together, these observations indicate that in the presence of IF2-GTP, the initiator tRNA recognizes the mRNA start codon in a conformation that is sensitive to inhibition by Ksg even in the mutant 30S subunits. By contrast, wild-type 30S subunits are much more sensitive than mutant ribosomes to Ksg when binding of initiator tRNA occurs at the classical P site²².

Template dependence of Ksg action

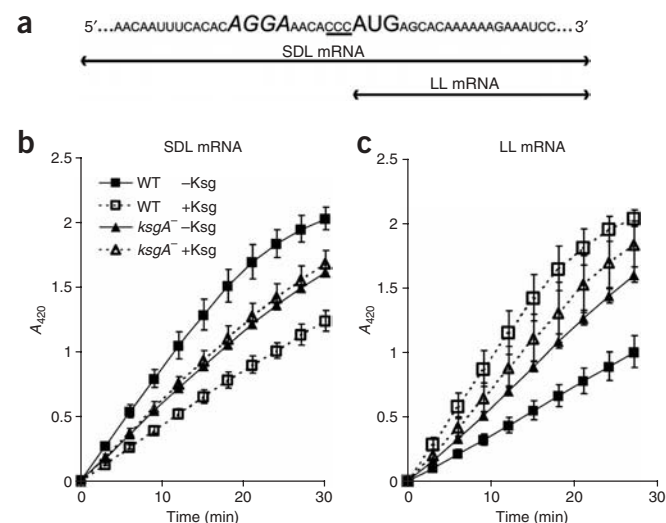
The above structural and biochemical results imply that hindrance of the mRNA pathway by Ksg could be responsible for Ksg inhibition of cell growth. Several lines of evidence also suggest that inhibition of translation by Ksg may be template dependent^{9,12,27}. In particular, Ksg inhibits translation of an mRNA carrying the 5' leader sequence of *lacZ* but not translation of its leaderless counterpart²⁷. To test the influence of the 5' leader on the inhibitory effect of Ksg, translation of mRNAs encoding β -galactosidase (β -gal), with or without a 5' leader sequence,

was measured in wild-type and Ksg-resistant mutant strains. The concentration of Ksg was kept as low as possible to avoid substantial inhibition of endogenous mRNAs (see Methods). In agreement with published results^{26,27}, Ksg largely inhibited translation of the fusion mRNA carrying the 5' leader sequence of *lacZ* (SDL mRNA) but did not inhibit translation of its leaderless equivalent (LL mRNA) (Fig. 5). In fact, the LL mRNA-driven β -gal activity considerably increased in the presence of Ksg in wild-type cells (Fig. 5c), as previously reported²⁷. In the Ksg-resistant mutants, production of β -gal from SDL mRNA was unaffected by Ksg (Fig. 5b). Notably, Ksg enhancement of LL mRNA-driven β -gal activity was considerably less in the resistant cells (Fig. 5c). These data support the idea that Ksg perturbs the interaction between the 5' leader sequences of SDL mRNAs and the ribosome during initiation, thereby arresting cell growth.

A 5' leader is not sufficient for inhibition by Ksg

To determine whether the 5' leader in an mRNA is necessary and sufficient for *in vivo* sensitivity to Ksg inhibition of translation, we tested translation of an mRNA encoding glutathione S-transferase (GST) but containing a different 5' leader from that in the *lacZ* sequence (Fig. 6)²⁸. To our surprise, Ksg did not inhibit translation of the GST mRNA in either wild-type or *ksgA*⁻ cells (Fig. 6a). In fact, Ksg considerably increased the synthesis of GST in wild-type cells but not in *ksgA*⁻ cells. As the GST mRNA carries a 5' leader containing a canonical Shine-Dalgarno sequence (Fig. 6b), this result was unexpected given the strong inhibition of SDL mRNA encoding β -gal, described above (Fig. 5b). In other words, the presence of a 5' leader is necessary but not sufficient for *in vivo* inhibition of natural mRNAs by Ksg. Notably, the 5' leader sequences of the SDL mRNA and the GST mRNA differ only in the nucleotides immediately preceding the AUG initiation codon (Figs. 5 and 6), indicating that Ksg may target mRNAs on the basis of sequences in or near the E site.

Figure 5 Effect of Ksg on β -gal synthesis. **(a)** Constructs used in β -gal assays. SDL, the 5' *lacZ* leader, carrying an SD sequence (enlarged, italic), is fused to *cl-lacZ*; LL, leaderless AUG-*cl-lacZ* construct (see Methods)⁴⁷. E-site triplet is underlined and start codon is enlarged. **(b,c)** Synthesis of β -gal from SDL mRNA **(b)** or LL mRNA **(c)** in wild-type (WT) strain JM101 or *ksgA*⁻ strain JM101 *ksgA*19 was induced by IPTG in the presence or absence of Ksg (50 $\mu\text{g ml}^{-1}$). Relative amounts of β -gal produced were determined by measuring activity of the fusion protein (A_{420} ; see Methods). Results shown are averages from three independent experiments. Error bars show s.d.



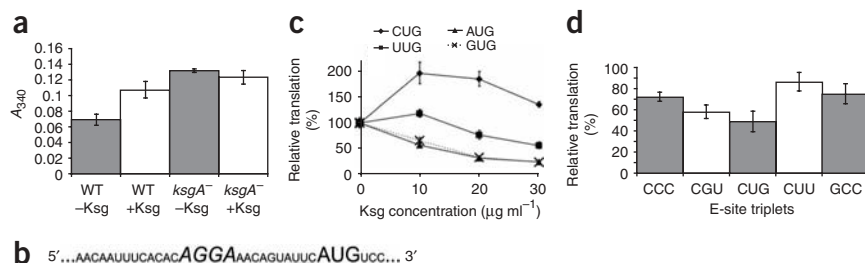


Figure 6 Dependence of inhibitory effect of Ksg on the primary sequence of the mRNA between positions -3 and +1. **(a)** Synthesis of GST driven by the GST mRNA encoded in pGEX-26 (ref. 28). GST synthesis was induced by IPTG in JM101 (WT) or JM101 ksgA19 (*ksgA*⁻) cells transformed with pGEX-26 in the presence or absence of Ksg (50 μg ml⁻¹). Initiation was monitored by measuring GST activity (*A*₃₄₀; see Methods). **(b)** Sequence of the GST leader in pGEX-26, formatted as in **Figure 5a**. **(c)** Inhibition of translation of SDL mRNA derivatives with different nucleotides at position +1 (NUG mRNAs), in the presence of increasing concentrations of Ksg. **(d)** Inhibition of translation of SDL mRNA derivatives with different E-site triplets, in the presence of 10 μg ml⁻¹ Ksg. All triplets were assayed in parallel. **a**, **c** and **d** show averages from three independent experiments. Error bars represent s.d.

Effect of the -3 to +1 sequence on Ksg inhibition

The above biochemical and structural data suggest that Ksg interacts with mRNA residues -3 to +1. This was tested by constructing SDL mRNA derivatives differing only in the sequence at these positions. In all four possible variants of position +1 (NUG mRNAs), the relative levels of β-gal activity reflected the strength of the codon-anticodon interaction during initiation, in agreement with published results (**Supplementary Fig. 2** online)²⁹. Consistent with the structural data (**Fig. 1e**), mutation of the first residue of the initiation codon considerably affected the extent of Ksg inhibition. Whereas purine start codons (AUG and GUG) were inhibited to similar extents by increasing concentrations of Ksg, pyrimidine start codons (UUG and CUG) gave higher relative levels of translation at low Ksg concentrations, with a gradual decrease at higher concentrations of Ksg (**Fig. 6c**). This effect was particularly acute for the CUG initiation codon, which showed an almost two-fold increase in β-gal activity at the lowest Ksg concentration tested and remained above the no-Ksg activity level at all other Ksg concentrations. The effect seems to be independent of the low β-gal activity of the mRNAs with pyrimidine start codons, as mRNAs with much lower activity but containing AUG start codons did not show this response to Ksg (data not shown). These results reveal the importance of position +1 of the mRNA for the extent of inhibition by Ksg, consistent with the predicted overlap of the inositol ring of Ksg with the backbone of mRNA at positions -1 and +1 (**Fig. 1e**).

The possible influence of residues -3 to -1 on the extent of Ksg inhibition revealed by the GST and SDL mRNAs was further analyzed with SDL mRNAs that carried different E-site triplets. To exclude possible interference of mRNA secondary structure, the triplets were chosen so that they would fold into the same predicted structures (data not shown). Again in agreement with the structural data, the E-site triplet had a substantial influence on the extent of inhibition by Ksg (**Fig. 6d**). In particular, changes at positions -1 and -2 resulted in the greatest shifts in β-gal activity in the presence of Ksg (**Fig. 6d**), within the set of mRNAs tested.

DISCUSSION

Early reports showed that Ksg binds both the 30S and 70S ribosome but not isolated 50S subunits³⁰. The ribosome structures presented here reveal the binding pocket for Ksg in the mRNA-binding cleft

of the 30S subunit between the head and the platform (**Fig. 1b**). The antibiotic is held in place by interactions with A794 and G926, the universally conserved nucleotides whose mutation confers high levels of Ksg resistance (**Fig. 1b,c** and **Supplementary Fig. 1**)^{19,31}. Binding of Ksg is also stabilized by residues A792, A1499, G1505 and U1506, which, together with A794 and G926, define the mRNA path in the P and E sites of the small ribosomal subunit (**Fig. 1c** and **Supplementary Fig. 1**). The other locus of Ksg resistance, the DASL^{16,19}, is not in direct contact with the antibiotic-binding pocket and probably confers resistance by an indirect mechanism that involves A792 (**Fig. 2a**).

Antibiotic resistance is often achieved by the loss of affinity for the drug as a result of mutation. However, Ksg-resistant ribosomes retain their ability to bind the antibiotic *in vitro* with an affinity that is not markedly

different from that of wild-type ribosomes (**Figs. 3** and **4**). Although our data and those of others¹⁰ show that mutant ribosomes can bind Ksg *in vitro*, these experiments cannot rule out the possibility that, at the intracellular Ksg levels, small affinity differences among the mutants could be responsible for resistance *in vivo*. However, it seems likely that the drug is bound to the mutant ribosomes *in vivo* for the following reasons. First, the highest concentration of Ksg used in the footprint assays (320 μg ml⁻¹) was an order of magnitude lower than the minimal inhibitory concentration (MIC, 3 mg ml⁻¹ or higher) for the A794G and G926A mutants¹⁹. Second, we observed that Ksg can inhibit the growth of the resistant strains under certain conditions *in vivo* (data not shown), indicating that the mutant ribosomes must bind the drug even at the intracellular concentrations.

Our results suggest that Ksg resistance functions similarly to streptomycin resistance and dependence, in that mutations in the ribosome compensate for drug interactions without the need to abrogate binding³². Should this be the case, Ksg-resistant ribosomes must be able to initiate translation in the presence of Ksg to support cell growth. A possible explanation for resistance would then be that initiation-complex formation could result in the displacement of Ksg from its binding pocket in Ksg-resistant ribosomes. This hypothesis best explains low-level resistance conferred by changes in the DASL, where cells are no longer resistant to Ksg once a concentration threshold is achieved¹⁹. For the strongest resistance mutations, those at A794 and G926 (ref. 19), the ribosome seems to work properly at extremely high concentrations of the drug (MIC value higher than 5mg ml⁻¹ for some of these mutants), as if normal ribosomal function were independent of the presence of the drug¹⁹. The most plausible mechanism to explain this would be that the mutations eliminate contacts of the ribosome with mRNA, Ksg or both, which alleviates the steric hindrance imposed on the mRNA as it travels through the mRNA channel occupied by Ksg. It is noteworthy that, although all mutants seem to follow a similar general trend in the assays reported here, we observed substantial differences among them (**Fig. 4a** and data not shown). Understanding how the different Ksg-resistance mutations distort the structure of the E site and its interaction with Ksg and the mRNA will be the focus of future studies.

According to our modeling of mRNA and P-site tRNA into the present structure (**Fig. 1e**)^{6,7,23}, inhibition of fMet-tRNA^{fMet} binding during initiation^{8,10,20} (**Fig. 4**) is probably due to potential steric

clashes of Ksg with the mRNA between positions -2 and $+1$. The structural data presented here help to explain the observation that Ksg inhibits translation of mRNAs with certain 5' leader sequences but not of leaderless mRNAs (Figs. 5 and 6)²⁷. As the mRNA sequence potentially subject to steric clash with Ksg is absent in leaderless mRNAs (from -2 to -1 , Fig. 1e), these mRNAs readily escape the inhibitory effect of the drug. The discrepancy between the *in vivo* resistance (Fig. 6)²⁷ and the *in vitro* sensitivity of T7-transcribed leaderless mRNAs in some of the assays (Fig. 5a)²⁶ may be due to the fact that the latter contain a 5'-pppG nucleotide in the -1 position³³. For mRNAs with 5' leader sequences, the extent of Ksg inhibition is highly dependent on the E-site triplet and, especially, on the identity of position $+1$ of the mRNA (Fig. 6). Start codons containing a purine at the $+1$ position can form either a canonical Watson-Crick or a wobble base pair with initiator tRNA, which would constrain the position of this base. By contrast, start codons containing a pyrimidine at the $+1$ position would introduce a mismatch that might substantially increase the flexibility of the mRNA backbone in this region. The results showing that Ksg allows mRNAs with UUG or CUG start codons to be translated far better, in relative terms, than mRNAs with AUG or GUG start codons (Fig. 6c), together with the experiments with different E-site triplets (Fig. 6d), strongly suggest that increased mRNA flexibility in this region can overcome the steric constraints induced by bound Ksg. Differential inhibition by Ksg of leadered mRNAs has also been reported in studies using polycistronic phage mRNAs^{9,12}.

According to the high-resolution 30S subunit and 70S ribosome structures, the conformation of the 30S platform is nearly invariant^{6,21}. During initiation, the platform would constrain the conformation of mRNA in the E site because of codon-anticodon base-pairing between mRNA and tRNA^{fMet} and the narrowing of the mRNA channel near positions -1 and $+1$, that is, between nucleotides G926 and A792 (refs. 6,7). Positions upstream of -3 in the mRNAs are disordered in the available structures^{6,7}, consistent with biochemical data indicating that the SD-antiSD helix formed between mRNA and the 3' end of 16S rRNA is decoupled from the E site³⁴. Therefore, the structure and flexibility of the mRNA in the E site could vary owing to spatial constraints on nucleotides -3 to -1 within the universally conserved E-site mRNA channel^{6,7,31} (Fig. 1e). A variable degree of mRNA flexibility in the E site, and probably in the area immediately upstream, downstream or both, could explain the influence of the E-site triplet on the extent of inhibition (Fig. 6a,d) and enhancement (Fig. 6a) of translation in the presence of Ksg. Biophysical measurements with natural mRNAs and Ksg will be necessary to test these ideas experimentally.

Variable mRNA structure and flexibility in the E site could also explain the importance of the E-site triplet during translation initiation. For example, it has been reported that the sequence of the triplet at the E site has a large effect (up to 20-fold) on translational activity^{4,5}. In the context of the SDL mRNAs used here, we observed an approximately 200-fold variation in β -gal activity (data not shown). Previous explanations for the influence of the 5' leader on the level of translation have focused mainly on the intramolecular (mRNA-mRNA) and intermolecular (mRNA-16S rRNA) Watson-Crick base-pairing potential of the mRNA sequence. The results reported here suggest that the structure adopted by mRNA in the E site may also have an important regulatory role. For example, after initial binding of the mRNA, whose affinity for the ribosome is mainly determined by the strength of the SD-antiSD interaction and the mRNA's ability to bind S1 (refs. 3,35-37), the probability of initiation-complex formation may be determined by the structure of the mRNA in the E site and its interaction with initiation factors. As a result, the

E site of the ribosome could serve as the final tuner of gene expression. This idea is consistent with the almost universal conservation of all the bases lining the E site³¹. Notably, a mechanism similar to the one described here may be exploited by eukaryotic mRNAs, as these mRNAs use their -5 to $+3$ sequence, the Kozak consensus sequence, to modulate the binding of the 40S subunit to the start codon during initiation of protein synthesis³⁸.

The surprising toeprinting results showing that Ksg inhibits IF2-GTP-fMet-tRNA^{fMet} binding even to Ksg-resistant 30S subunits (Fig. 4a and Supplementary Table 3) support the idea that the mRNA channel near the -1 and $+1$ positions is highly constrained. The results are in agreement with previous reports showing that Ksg inhibits the IF2-directed binding of initiator tRNA to Ksg-resistant 30S subunits from *ksgA* mutants¹⁰. Together, the available evidence reveals that, in the presence of IF2-GTP, the initiator tRNA must bind the 30S subunit in a conformation that introduces a stronger steric clash with Ksg than during the IF-independent binding of this tRNA at the classical P site of Ksg-resistant ribosomes (Fig. 4b and Supplementary Table 3)²². Recent cryo-EM reconstructions of 70S initiation complexes in the presence of IFs and the nonhydrolyzable GTP analog GMPPNP³⁹ have shown that initiator tRNA is delivered to the ribosome at a previously uncharacterized site termed P/I (P site on the 30S subunit, new position 'I' on the 50S subunit). Repositioning of the initiator tRNA from the P/I site to the classical P site, after hydrolysis of GTP, requires rotation in the plane of the tRNA by 20° about the anticodon loop³⁹. Binding of the initiator tRNA at the P/I site could explain the results of the toeprint experiments with 30S subunits and IF2-GTP-fMet-tRNA^{fMet} (Fig. 4a and Supplementary Table 3). As the mutant ribosomes are Ksg resistant *in vivo*, additional elements present during initiation *in vivo* and missing in the toeprint assays, such as 5' leader sequences, the 50S subunit and IF3, could be responsible for abrogating the inhibitory effect of Ksg on initiation-complex formation via the P/I site. Future experiments will be needed to determine how Ksg affects initiation-complex formation in the P/I and classical P/P states.

METHODS

Bacterial strains. *E. coli* $\Delta 7$ strains AVS69009 pKK C1192U (wild type), AVS69022 pKK 1192U (*ksgA19*), AVS69009 pKK C1192U-A794G, AVS69009 pKK C1192U-G926A and AVS69009 pKK C1192U-A1519C have been described¹⁹.

Crystallographic analysis. *E. coli* ribosomes were purified and crystallized as described²¹. The crystals were stabilized in 20% (v/v) 2-methyl-2,4-pentanediol (MPD), 20 mM HEPES (pH 7.5), 28 mM MgCl₂, 350 mM NH₄Cl, 1 mM spermine, 0.5 mM spermidine, 3% (w/v) PEG 8,000 and 24% (w/v) PEG 400, then soaked in a solution containing 1 mg ml⁻¹ Ksg (Wako, 11-00523). Diffraction data were measured, integrated and scaled as described²¹ (Supplementary Table 1). Difference electron density maps were calculated using the observed amplitudes from the 70S ribosome-Ksg crystal diffraction, minus the amplitudes of the apo-70S ribosome crystal diffraction. We derived structure-factor phases from the model of the apo-70S ribosome, then performed density modification using Pirata^{21,40,41} (Supplementary Table 1). The coordinates of the X-ray structure of Ksg⁴² served to create an initial starting model for the drug using ArgusLab⁴³.

After docking, the 70S-Ksg models were refined against the crystallographic data using CNS⁴⁰ (Supplementary Table 1). Superposition of the present 70S ribosome structure with those of the *Thermus thermophilus* 30S ribosome (PDB entries 1J5E and 1FJG) was done in O⁴⁴ by selecting a subset of atoms in the platform of the subunit, namely 16S rRNA residues 922-930 and 790-796. The final r.m.s. deviation was 0.441 Å.

Ksg footprinting experiments. Ribosomal subunits were prepared as described⁴⁵ from all the above $\Delta 7$ strains. We used 30 pmol of 30S subunits in chemical modification reactions set up as described²⁰ at Ksg (Fluka)

concentrations of 64 $\mu\text{g ml}^{-1}$ and 320 $\mu\text{g ml}^{-1}$. The sites of chemical modification were identified as described⁴⁶.

Toeprint analysis. Primer-extension inhibition analysis with leaderless T7 transcripts was done as described⁴⁷. We incubated 5 pmol of 30S subunits with or without 5 pmol of 50S subunits at 37 °C for 15 min in reaction buffer (10 mM Tris-HCl (pH 7.4), 60 mM NH_4Cl , 10 mM magnesium acetate, 6 mM β -mercaptoethanol). The ribosomes were added to a mixture containing 1 pmol of preannealed LL mRNA–primer complex and the following components, as specified in the figure legends: 15 pmol of tRNA^{Met} or fMet- tRNA^{Met} , 10 pmol IF2, 0.5 mM GTP and Ksg (Fluka) in a final volume of 15 μl .

Primer-extension analysis of 16S rRNA. Plasmid-encoded ribosomes carrying mutations in the m_2A stem-loop, isolated in both the wild-type and ksgA^- backgrounds, were subjected to primer extension as described¹⁹.

In vivo Ksg inhibition assays. The following constructs have been described^{29,47}: SDL-AUG-cl-*lacZ* (SDL) carrying a leadered cl-*lacZ* fusion; LL-AUG-cl-*lacZ* (LL), carrying a leaderless cl-*lacZ* fusion; and the pSD-NUGcl set of plasmids, encoding the alternative start codons CUG, GUG and UUG. The constructs carrying different E-site triplets were built by PCR-directed randomization of the –1 triplet (E site) in the leadered cl-*lacZ* fusion plasmid pSD-AUG-cl²⁹. The plasmids were transformed into strains JM101 and JM101 ksgA19 (ref. 19) as indicated. For the experiments of **Figure 4** and **Figure 6a**, the cultures were grown in minimal medium supplemented with 0.2% (w/v) Casamino acids and 0.2% (w/v) glucose, to $A_{600} = 0.4$. After induction with 1 mM IPTG (final concentration), half of the cultures were transferred to new flasks to which Ksg (Fluka) was added to a final concentration of 50 $\mu\text{g ml}^{-1}$, far below the MIC for wild-type cells (80–150 $\mu\text{g ml}^{-1}$)¹⁹. Cultures were grown for an additional 3 h, chilled quickly on ice and harvested. The cell pellets were resuspended in 1 ml of PBS with 0.45% (w/v) Brij58 and 0.15% (w/v) deoxycholate, and lysed by repeated quick freeze-thaw in an ethanol–dry ice bath. Lysates were cleared by centrifugation and the amount of total protein was determined for normalization purposes. Note that about 30 times more lysate was loaded in the assays with LL mRNA than in the assays with SDL mRNA. For the assays in **Figure 6c,d**, cells were grown in minimal medium containing 0.2% (w/v) maltose (as carbon source) and 25 $\mu\text{g ml}^{-1}$ kanamycin to approximately $A_{600} = 0.3$. After induction with 1 mM IPTG, the cultures were divided into flasks containing the same medium supplemented with Ksg (Sigma, K-1253), as indicated, and assayed for β -gal 3 h later. β -gal and GST activities were assayed as described^{28,48}.

Accession codes. Protein Data Bank: Coordinates for two 70S ribosomes have been deposited with accession codes 1VS5 (ribosome 1, 30S subunit), 1VS6 (ribosome 1, 50S subunit), 1VS7 (ribosome 2, 30S subunit) and 1VS8 (ribosome 2, 50S subunit).

Note: Supplementary information is available on the Nature Structural & Molecular Biology website.

ACKNOWLEDGMENTS

We thank K. Frankel, G. Hura and J. Holton for help with data measurements at the SIBYLS beamline at the Advanced Light Source. A.V.-S. would like to acknowledge I. Tinoco for valuable discussions, C.M. Brown for help with Transterm and F. Vila for balance and coherence. This work was funded by the US National Institutes of Health (GM65050 to J.H.D.C., GM065120 to G.R.J., GM19756 to A.E.D. and National Cancer Institute grant CA92584 for the SIBYLS and 8.3.1 beamlines) and by the US Department of Energy (DE-AC03-76SF00098, KP110201 and LBNL LDRD 366851 to J.H.D.C. and DE-AC03 76SF00098 for the SIBYLS and 8.3.1 beamlines).

COMPETING INTERESTS STATEMENT

The authors declare that they have no competing financial interests.

Published online at <http://www.nature.com/nsmb/>

Reprints and permissions information is available online at <http://npg.nature.com/reprintsandpermissions/>

1. Laursen, B.S., Sorensen, H.P., Mortensen, K.K. & Sperling-Petersen, H.U. Initiation of protein synthesis in bacteria. *Microbiol. Mol. Biol. Rev.* **69**, 101–123 (2005).

- Kozak, M. Regulation of translation via mRNA structure in prokaryotes and eukaryotes. *Gene* **361**, 13–37 (2005).
- Boni, I.V., Isaeva, D.M., Musychenko, M.L. & Tzareva, N.V. Ribosome-messenger recognition: mRNA target sites for ribosomal protein S1. *Nucleic Acids Res.* **19**, 155–162 (1991).
- Hui, A., Hayflick, J., Dinkelspiel, K. & de Boer, H.A. Mutagenesis of the three bases preceding the start codon of the beta-galactosidase mRNA and its effect on translation in *Escherichia coli*. *EMBO J.* **3**, 623–629 (1984).
- Matteucci, M.D. & Heyneker, H.L. Targeted random mutagenesis: the use of ambiguously synthesized oligonucleotides to mutagenize sequences immediately 5' of an ATG initiation codon. *Nucleic Acids Res.* **11**, 3113–3121 (1983).
- Carter, A.P. *et al.* Functional insights from the structure of the 30S ribosomal subunit and its interactions with antibiotics. *Nature* **407**, 340–348 (2000).
- Yusupova, G.Z., Yusupov, M.M., Cate, J.H. & Noller, H.F. The path of messenger RNA through the ribosome. *Cell* **106**, 233–241 (2001).
- Okuyama, A., Machiyama, N., Kinoshita, T. & Tanaka, N. Inhibition by kasugamycin of initiation complex formation on 30S ribosomes. *Biochem. Biophys. Res. Commun.* **43**, 196–199 (1971).
- Okuyama, A. & Tanaka, N. Differential effects of aminoglycosides on cistron-specific initiation of protein synthesis. *Biochem. Biophys. Res. Commun.* **49**, 951–957 (1972).
- Poldermans, B., Goosen, N. & Van Knippenberg, P.H. Studies on the function of two adjacent N6,N6-dimethyladenosines near the 3' end of 16 S ribosomal RNA of *Escherichia coli*. I. The effect of kasugamycin on initiation of protein synthesis. *J. Biol. Chem.* **254**, 9085–9089 (1979).
- Tai, P.C., Wallace, B.J. & Davis, B.D. Actions of aurintricarboxylate, kasugamycin, and pactamycin on *Escherichia coli* polysomes. *Biochemistry* **12**, 616–620 (1973).
- Kozak, M. & Nathans, D. Differential inhibition of coliphage MS2 protein synthesis by ribosome-directed antibiotics. *J. Mol. Biol.* **70**, 41–55 (1972).
- Umezawa, H., Hamada, M., Suhara, Y., Hashimoto, T. & Ikekawa, T. Kasugamycin, a new antibiotic. *Antimicrob. Agents Chemother.* **5**, 753–757 (1965).
- Ishigami, J., Fukuda, Y. & Hara, S. Clinical use of Kasugamycin for urinary tract infections due to *Pseudomonas aeruginosa*. *J. Antibiot. [B]* **20**, 83–84 (1967).
- Sparling, P.F. Kasugamycin resistance: 30S ribosomal mutation with an unusual location on the *Escherichia coli* chromosome. *Science* **167**, 56–58 (1970).
- Helser, T.L., Davies, J.E. & Dahlberg, J.E. Mechanism of kasugamycin resistance in *Escherichia coli*. *Nat. New Biol.* **235**, 6–9 (1972).
- Baan, R.A. *et al.* High-resolution proton magnetic resonance study of the secondary structure of the 3'-terminal 49-nucleotide fragment of 16S rRNA from *Escherichia coli*. *Proc. Natl. Acad. Sci. USA* **74**, 1028–1031 (1977).
- O'Farrell, H.C., Scarsdale, J.N. & Rife, J.P. Crystal structure of KsgA, a universally conserved rRNA adenine dimethyltransferase in *Escherichia coli*. *J. Mol. Biol.* **339**, 337–353 (2004).
- Vila-Sanjurjo, A., Squires, C.L. & Dahlberg, A.E. Isolation of kasugamycin resistant mutants in the 16 S ribosomal RNA of *Escherichia coli*. *J. Mol. Biol.* **293**, 1–8 (1999).
- Woodcock, J., Moazed, D., Cannon, M., Davies, J. & Noller, H.F. Interaction of antibiotics with A- and P-site-specific bases in 16S ribosomal RNA. *EMBO J.* **10**, 3099–3103 (1991).
- Schuwirth, B.S. *et al.* Structures of the bacterial ribosome at 3.5 Å resolution. *Science* **310**, 827–834 (2005).
- Moazed, D. & Noller, H.F. Binding of tRNA to the ribosomal A and P sites protects two distinct sets of nucleotides in 16 S rRNA. *J. Mol. Biol.* **211**, 135–145 (1990).
- Yusupov, M.M. *et al.* Crystal structure of the ribosome at 5.5 Å resolution. *Science* **292**, 883–896 (2001).
- Cunningham, P.R. *et al.* Site-specific mutation of the conserved m_2^6A m_2^6A residues of *E. coli* 16S ribosomal RNA. Effects on ribosome function and activity of the ksgA methyltransferase. *Biochim. Biophys. Acta* **1050**, 18–26 (1990).
- Vila-Sanjurjo, A. & Dahlberg, A.E. Mutational analysis of the conserved bases C1402 and A1500 in the center of the decoding domain of *Escherichia coli* 16 S rRNA reveals an important tertiary interaction. *J. Mol. Biol.* **308**, 457–463 (2001).
- Moll, I. & Blasi, U. Differential inhibition of 30S and 70S translation initiation complexes on leaderless mRNA by kasugamycin. *Biochem. Biophys. Res. Commun.* **297**, 1021–1026 (2002).
- Chin, K., Shean, C.S. & Gottesman, M.E. Resistance of lambda cl translation to antibiotics that inhibit translation initiation. *J. Bacteriol.* **175**, 7471–7473 (1993).
- Andre, A. *et al.* Reinitiation of protein synthesis in *Escherichia coli* can be induced by mRNA cis-elements unrelated to canonical translation initiation signals. *FEBS Lett.* **468**, 73–78 (2000).
- O'Donnell, S.M. & Janssen, G.R. The initiation codon affects ribosome binding and translational efficiency in *Escherichia coli* of cl mRNA with or without the 5' untranslated leader. *J. Bacteriol.* **183**, 1277–1283 (2001).
- Okuyama, A., Tanaka, N. & Komai, T. The binding of kasugamycin to the *Escherichia coli* ribosomes. *J. Antibiot. (Tokyo)* **28**, 903–905 (1975).
- Cannone, J.J. *et al.* The comparative RNA web (CRW) site: an online database of comparative sequence and structure information for ribosomal, intron, and other RNAs. *BMC Bioinformatics* **3**, 2 (2002).
- Allen, P.N. & Noller, H.F. Mutations in ribosomal proteins S4 and S12 influence the higher order structure of 16 S ribosomal RNA. *J. Mol. Biol.* **208**, 457–468 (1989).
- Lowary, P., Sampson, J., Milligan, J., Groebe, D. & Uhlenbeck, O.C. in *Structure and dynamics of RNA* (eds Knippenberg, P.H. & Hilbers, C.W.) 69–76 (Plenum, New York, 1986).

34. Marquez, V., Wilson, D.N., Tate, W.P., Triana-Alonso, F. & Nierhaus, K.H. Maintaining the ribosomal reading frame: the influence of the E site during translational regulation of release factor 2. *Cell* **118**, 45–55 (2004).
35. Shine, J. & Dalgarno, L. The 3'-terminal sequence of *Escherichia coli* 16S ribosomal RNA: complementarity to nonsense triplets and ribosome binding sites. *Proc. Natl. Acad. Sci. USA* **71**, 1342–1346 (1974).
36. Calogero, R.A., Pon, C.L., Canonaco, M.A. & Gualerzi, C.O. Selection of the mRNA translation initiation region by *Escherichia coli* ribosomes. *Proc. Natl. Acad. Sci. USA* **85**, 6427–6431 (1988).
37. Studer, S.M. & Joseph, S. Unfolding of mRNA secondary structure by the bacterial translation initiation complex. *Mol. Cell* **22**, 105–115 (2006).
38. Kozak, M. At least six nucleotides preceding the AUG initiator codon enhance translation in mammalian cells. *J. Mol. Biol.* **196**, 947–950 (1987).
39. Allen, G.S., Zavialov, A., Gursky, R., Ehrenberg, M. & Frank, J. The cryo-EM structure of a translation initiation complex from *Escherichia coli*. *Cell* **121**, 703–712 (2005).
40. Brunger, A.T. *et al.* Crystallography & NMR system: a new software suite for macromolecular structure determination. *Acta Crystallogr. D Biol. Crystallogr.* **54**, 905–921 (1998).
41. Cowtan, K. General quadratic functions in real and reciprocal space and their application to likelihood phasing. *Acta Crystallogr. D Biol. Crystallogr.* **56**, 1612–1621 (2000).
42. Ikekawa, T., Umezawa, H. & Iitaka, Y. The structure of kasugamycin hydrobromide by x-ray crystallographic analysis. *J. Antibiot. (Tokyo)* **19**, 49–50 (1966).
43. Thompson, M.A. ArgusLab 4.0.1 (Planaria Software, Seattle, 2004).
44. Jones, T.A., Zou, J.Y., Cowan, S.W. & Kjeldgaard, M. Improved methods for building protein models in electron density maps and the location of errors in these models. *Acta Crystallogr. A* **47**, 110–119 (1991).
45. Vila, A., Viril-Farley, J. & Tappich, W.E. Pseudoknot in the central domain of small subunit ribosomal RNA is essential for translation. *Proc. Natl. Acad. Sci. USA* **91**, 11148–11152 (1994).
46. Vila-Sanjurjo, A. *et al.* X-ray crystal structures of the WT and a hyper-accurate ribosome from *Escherichia coli*. *Proc. Natl. Acad. Sci. USA* **100**, 8682–8687 (2003).
47. Van Etten, W.J. & Janssen, G.R. An AUG initiation codon, not codon-anticodon complementarity, is required for the translation of unleadered mRNA in *Escherichia coli*. *Mol. Microbiol.* **27**, 987–1001 (1998).
48. Miller, J.H. *A Short Course in Bacterial Genetics* (Cold Spring Harbor Laboratory Press, Cold Spring Harbor, New York, USA, 1991).

Copyright of Nature Structural & Molecular Biology is the property of Nature Publishing Group and its content may not be copied or emailed to multiple sites or posted to a listserv without the copyright holder's express written permission. However, users may print, download, or email articles for individual use.